A K-feldspar–liquid hygrometer specific to alkaline differentiated magmas

Silvio Mollo[1], Matteo Masotta[2], Francesca Forni[3], Olivier Bachmann[3], Gianfilippo De Astis[1], Gordon Moore[4], Piergiorgio Scarlato[1]

[1] Istituto Nazionale di Geofisica e Vulcanologia, Roma, Italy

[2] Bayerisches Geoinstitut, Universität Bayreuth, Bayreuth, Germany

[3] Department of Earth Sciences, Institute of Geochemistry and Petrology, ETH, Zurich, Switzerland

[4] Department of Earth and Environmental Sciences, University of Michigan, MI, USA

Corresponding author:

Silvio Mollo

Istituto Nazionale di Geofisica e Vulcanologia

Via di Vigna Murata 605

00143 ROMA - ITALY

office tel. +39 0651860674

fax +39 0651860507

e-mail mollo@ingv.it

Abstract

We present a K-feldspar–liquid hygrometer specific to alkaline differentiated magmas that is calibrated through the regression analysis of sanidine and anorthoclase crystals coexisting with trachyte and phonolite melts. Partial-regression leverage plots were used to determine the minimum number of regression parameters that closely describe the variance of the dataset. The derived model was tested using K-feldspar–liquid pairs not included into the calibration dataset in order to address issues of systematic errors. When K-feldspar and plagioclase crystals coprecipitate from the same alkaline liquid under identical P-T-X-fO_2-H_2O conditions, the ability prediction of the new hygrometer is comparable to that of previous plagioclase–liquid models. To minimize the error of H_2O estimate caused by the inadvertent use of disequilibrium data in natural samples, we have also calibrated a new test for equilibrium based on Or–Ab exchange between K-feldspar and coexisting melt. As an immediate application for both equilibrium and hygrometer models, we used as input data K-feldspar–liquid pairs from alkaline explosive eruptions at the Phlegrean Fields. The estimates of H_2O dissolved in natural trachyte and phonolite magmas closely match those determined by melt inclusion analysis and H_2O solubility modeling. This leads to the conclusion that our new models can significantly contribute to a better quantitative characterization of the H_2O content in differentiated alkaline magmas feeding large-volume explosive eruptions.

Keywords: hygrometer; K-feldspar; phonolite; trachyte; Phlegrean Fields

1. Introduction

Over the years, several hygrometers have been constructed using plagioclase-liquid exchange between anorthite and albite components (Housh and Luhr 1991; Putirka 2005, 2008; Lange et al. 2009). These models are widely applied because of the ubiquitous crystallization of plagioclase in basalts through rhyolites over a large range of temperatures, pressures, and H_2O concentrations. However, in alkaline differentiated magmas, the stability of plagioclase is drastically reduced or suppressed due to abundant K-feldspar crystallization. For example, the plagioclase:K-feldspar ratio in trachytes is 1:10 or even lower, whereas plagioclase is frequently lacking in phonolites (e.g., Ablay et al., 1995; Fulignati et al., 2004). Under crustal pressures (0.1-0.3 GPa), K-feldspar typically equilibrates at temperatures lower than those of olivine, clinopyroxene and magnetite, but H_2O exsolution from 7 to 2 wt.% increases the K-feldspar first appearance from 800 to 925 °C (Andujar et al., 2010). The overall crystal content of trachytic and phonolitic magmas remains lower than 7 wt.% until K-feldspar crystallizes and then the crystallinity increases up to 50 wt.% due to prevalent K-feldspar formation (Andujar et al., 2008, 2010; Andujar and Scaillet 2012). As a result, the magmatic system undergoes important chemical and physical changes and the amount of H_2O dissolved in magma drastically increases (Fowler et al., 2007), potentially leading to violent explosive eruptions and voluminous caldera-forming events (e.g., Pappalardo et al., 2008; Palladino et al., 2014).

Since H_2O is one of the most important parameters setting the stage for highly explosive eruptions, we present in this study a new K-feldspar–liquid hygrometer specific to alkaline differentiated magmas. The calibration dataset consists of sanidine and anorthoclase in equilibrium with trachytic and phonolitic liquids. Tests performed on a sample population of the dataset demonstrate the reliability of the new hygrometer in predicting melt-H_2O contents. To minimize the error of estimate caused by the accidental use of disequilibrium data, a new equilibrium model between K-feldspar and coexisting liquid has been also calibrated and tested. Both the new hygrometer and equilibrium models are reported into a spreadsheet available online as

supplementary material. Application to explosive eruptive products at the Phlegrean Fields provides values that closely match with H_2O contents measured in melt inclusions and through the modelling of H_2O solubility in trachytic and phonolitic magmas.

2. Dataset, component calculation and regression strategy

The dataset used to calibrate both the new hygrometer and equilibrium models consists of K-feldspar–liquid pairs obtained through phase equilibrium experiments on alkaline differentiated magmas (Table 1EA). Experimental data from previous studies encompass the range of conditions P=0.05-0.30 GPa, T=725-950 °C, H_2O=2.7-9.5 wt.% and fO_2=QFM–NNO+1.5 (i.e., Fabbrizio and Carroll 2008; Andujar et al. 2008, 2010; Andujar and Scaillet 2012; Masotta et al., 2013). On the whole, the calibration dataset comprises a wide range of trachyte and phonolite melts (SiO_2 = 57-69 wt.% and Na_2O+K_2O = 10-16 wt.%; Fig. 1a) in equilibrium with sanidine and anorthoclase feldspars (Ab_{16-71}, An_{0-12} and Or_{19-84}; Fig. 1b).

Component calculations were performed following the procedure reported by Putirka (2008). Liquid components have been treated as cation fractions of the oxides SiO_2, TiO_2, $AlO_{1.5}$, FeO, MnO, MgO, CaO, $NaO_{0.5}$, $KO_{0.5}$, and $PO_{2.5}$. The H_2O content was excluded from the calculation and was added to the models in units of wt.%. The amounts of K-feldspar components were calculated from cation fractions as $An^{kfs} = [Ca/(Ca + Na + K)]^{kfs}$, $Ab^{kfs} = [Na/(Ca + Na + K)]^{kfs}$, and $Or^{kfs} = [K/(Ca + Na + K)]^{kfs}$.

A number of regression analyses were performed to derive new and more precise hygrometer and equilibrium models. The dependent variable was plotted versus the cation fractions of both liquid and feldspar with the aim to capture regression parameters with the highest degrees of correlation (Table 1). As a result of these plots, we selected independent variables with high correlation coefficients (R) and low standard errors of estimate (SEE) (Table 2). To improve the model prediction, more complex and statistical significant independent variables for liquid, K-feldspar and K-feldspar-liquid exchange were also considered for the multiple linear regression

analysis, e.g., $\ln[Si\times(Ti+Mg)]^{liq}$, $\ln[(Si\times Ca)/(Fe+Ca)^2]^{Kfs}$ and $\ln[(Or^2)^{Kfs}/(Ca\times K)^{liq}]$ (Tables 1 and 2). This made possible to obtain regression slope and intercept for calculated versus measured values that most closely approach to one and zero, respectively. The predictive model was developed including only those independent variables that closely described the variance of the dataset (cf. Putirka et al. 1999), whereas all variables producing data overfitting were removed from the regression analysis (Jefferys and Berger 1992; Ratkowsky 1990). Therefore, parameters used for the multiple linear regression analysis were the minimum number of independent variables required to explain the observed variability (Table 2). Through the statistical formula for the standardized regression coefficient, we also determined the influence of each independent variable on the ability prediction of the model; specifically, the standardized regression coefficient equals to the standard deviation of the independent variable (Table 1) multiplied by the standard deviation of the dependent variable (Table 1) and divided by the regression coefficient of the independent variable (Table 2).

The new hygrometer was tested by means of two independent datasets not included into the original calibration dataset (Table 1EA). The first dataset consists of phase equilibrium compositions subtracted to the calibration dataset and obtained in laboratory by the same authors (i.e., Fabbrizio and Carroll 2008; Andujar et al. 2008, 2010; Andujar and Scaillet 2012; Masotta et al., 2013). The second dataset comprises K-feldspar–liquid pairs recovered through MELTS (Ghiorso and Sack, 1995) numerical simulations that were carried out at P-T-H_2O-fO_2 conditions comparable to those of laboratory experiments, i.e., 0.10-0.30 GPa, 786-1007 °C, 1.8-8.0 wt.% H_2O and QFM–NNO+0.5 buffers (Table 1EA). This latter test was encouraged by recent studies that demonstrated a fairly good agreement between phase relationships and compositions predicted by MELTS and those observed in natural and experimental trachyte and phonolite products (e.g., Fowler et al., 2007; Masotta et al., 2010). The MELTS code is based on an independent set of thermodynamic data for mineral phases and its outputs are the result of thermodynamic algorithms for detection of phase saturation and energy convergence (e.g., Gibbs free energy minimization;

Ghiorso and Sack, 1995). Conversely, empirical models coincide with the fit of laboratory data that are used to retrieve statistically significant regression parameters (cf. Putirka 2008). In view of these very different kinds of calibrations, Armienti et al (2013) suggested that the convergence between MELTS and empirical models and their independent estimates of melt-H_2O contents is a useful test to assess whether or not both models are internally consistent.

We also determined the error of H_2O estimate (EWE) caused by the inclusion of rhyolitic data that are significantly different from the trachytic and phonolitic compositions recommended for the new hygrometer. According to previous studies, EWE is expressed as the difference between the concentration of H_2O measured in the melt and that predicted by the model (Putirka, 2008; Masotta et al., 2013; Mollo et al., 2013). This test is very useful to ascertain the limits of the model and to evaluate the uncertainty that should be expected by the use of highly evolved K-feldspar-liquid pairs.

3. Results and discussion

3.1 Calibration, test, and limit of the hygrometer

With respect to the liquid components, i.e., Al^{liq}, Fe^{liq}, Ca^{liq} and Na^{liq}, used for the calibration of previous plagioclase-liquid hygrometers (i.e., Putirka, 2005, 2008 and Lange et al., 2009), results from our liner regression fits suggest that Si^{liq}, Ti^{liq} and Mg^{liq} are more appropriate to predict the amount of H_2O dissolved in differentiated alkaline magmas (Table 1). These regression data also indicate that Si^{kfs}, Fe^{kfs} and Ca^{kfs} are the most suitable predictors for K-feldspar components (Table 1). Noteworthy, the correlation coefficient exhibits a maximum value of 0.55 for the liquid and 0.66 for the K-feldspar when these parameters are expressed as $[Si/(Ti+Mg)]^{liq}$ and $[(Si\times Ca)/(Fe+Ca)^2]^{kfs}$, respectively (Table 1). For the example of the hygrometer of Putirka (2005), the introduction of a plagioclase-liquid parameter based on An^{pl}, Ca^{liq} and Na^{liq} contributed to reduce significantly the uncertainty of the model. Due to the different Ca-Na-K proportions in K-feldspars and alkaline differentiated liquids, this parameter did not offer any improvement for the

regression statistics of the new hygrometer as well as no improvements were found through the use of single An, Ab and Or parameters (Table 1). Conversely, the new K-feldspar-liquid parameter based on Or^{Kfs}, Ca^{liq} and K^{liq} shows a fairly good correlation (R^2 = 0.63) with the concentration of H_2O in the melt (Table 1). According to the observation of Putirka (2005, 2008), there is a negligible effect of pressure on H_2O prediction (Table 1). In this respect, thermodynamic data of Lange et al. (2009) indicate a minimal influence of pressure on the solid-liquid exchange reaction due to the fact that ±100 MPa leads to an uncertainty of only ±0.1 wt.% H_2O. In contrast, the temperature of the system is highly correlated (R^2 = 0.51) with the melt-H_2O content being one of the most important predictive factors (Table 1). On the whole, liquid, K-feldspar and K-feldspar-liquid independent variables are successfully described by the following multiple linear regression model:

$$H_2O(wt.\%) = -a + b\frac{10^4}{T(^\circ C)} - c\ln\left[Si(Ti+Mg)\right]^{liq} + d\ln\left[\frac{(Or^2)^{kfs}}{(CaK)^{liq}}\right] + e\ln\left[\frac{(SiCa)}{(Fe+Ca)^2}\right]^{kfs}$$

(Eqn. 1)

Table 2 reports the statistical values and regression coefficients of Eqn. (1). Fig. 2a shows the very good alignment between measured and predicted H_2O values. The standard error of estimate of Eqn (1) is slightly reduced ~0.4 wt.% H_2O with respect to that (SEE = 1.1 wt.% H_2O) of models of Putirka (2005; 2008), but it is still ~0.4 wt.% H_2O higher than that (SEE = 0.32 wt.% H_2O) of the model of Lange et al. (2009). The relative effect of predictors on the estimate of melt-H_2O concentration is 32%, 27%, 23% and 18% for temperature, liquid, K-feldspar-liquid and K-feldspar, respectively. Therefore, 68% of the predictive power of the hygrometer is due to the effect of liquid and K-feldspar components, excluding the possibility that estimates from Eqn. (1) are heavily controlled by the temperature of the system (cf. Mollo et al., 2011a).

In order to verify the accuracy of Eqn. (1), K-feldspar–liquid pairs from experiments and MELTS simulations not included into the calibration dataset were used as test compositions (Table 1EA). Results from the regression analysis indicate that the new hygrometer successfully reproduces the melt-H_2O content. Moreover, R^2 and SEE calculated for both experimental (Fig. 2b) and MELTS (Fig. 2c) datasets exhibit almost identical values. This finding ensures that (1) no systematic overestimates or underestimates were due to mis-calibration and (2) the number of model parameters did not cause data overfitting. As an additional test, we have also recalibrated Eqn. (1) through the global regression analysis of both calibration and test data (Fig. 2d). The predictive power of the model is weakly improved and the uncertainty slightly decreases from 0.75 to 0.53 wt.% H_2O (Table 2). However, regression-derived coefficients of the recalibrated Eqn. (1) do not differ significantly from those of the original calibration (Table 2), suggesting that the hygrometer is consistent with K-feldspar and liquid compositions obtained in laboratory and those derived by MELTS thermodynamic standard-state reactions.

One of the most important limitations of models obtained through regression analysis of empirical data is represented by the P-T-X-H_2O bounds of the calibration dataset (Putirka, 2008; Mollo et al., 2010a, b). In this view, Masotta et al. (2013) observed how the use of models outside their calibration bounds produces uncertainties that are sometimes very large. To assess the extent of this limitation, we have used as input data for the new hygrometer experimental sanidine and anorthoclase crystals (An_{0-15}, Ab_{10-74}, and Or_{25-83}) in equilibrium with rhyolitic liquids (SiO_2 = 70-77 wt.% and Na_2O+K_2O = 5-11 wt.%) at P=0.02-0.15 GPa, T=678-925 °C, H_2O=0.41-7.94 wt.% and fO_2=QFM–NNO+2 (Scaillet and MacDonald, 2003; Di Carlo et al., 2010; see Table 2EA). Fig. 3 shows EWE calculated for each K-feldspar-liquid and plotted versus the corresponding rhyolitic liquid composition expressed as $[Si/(Na+K)]^{liq}$. As a term of comparison, EWE calculated for trachytic and phonolitic compositions from the test dataset is also plotted in Fig. 3. Generally, EWE progressively increases with increasing $[Si/(Na+K)]^{liq}$ (Fig. 3) due to the fact that in the $NaA1SiO_4$-$KA1SiO_4$-SiO_2-H_2O system (Bowen, 1937; Hamilton and MacKenzie, 1965) a trachytic magma can

evolve either towards phonolite or alkaline rhyolite producing undersaturated and oversaturated liquids, respectively. The uncertainty measured for trachytic and phonolitic magmas is rationally low (EWE = 0.01-1.44 wt.% H_2O), but rhyolitic compositions leads to strong overestimates (EWE = 1.40-11.50 wt.% H_2O) that can be two times higher than the maximum solubility of H_2O (i.e. ~5.2 wt.%; Holtz et al., 2001). This leads to the conclusion that caution must be taken in using K-feldspar-liquid pairs different from those of the calibration dataset of the new hygrometer.

3.2 Plagioclase–liquid versus K-feldspar–liquid hygrometer

The new hygrometer faithfully predicts the amount of H_2O dissolved in phonolitic and trachytic magmas and, in principle, the estimate must be consistent with that obtained using plagioclase hygrometer, whenever both plagioclase and K-feldspar coprecipitate from the same host magma. To test this hypothesis, we must be certain that plagioclase and K-feldspar are simultaneously crystallizing over the effect of identical P-T-H_2O-fO_2 conditions. This is made possible by the selection of MELTS runs in which plagioclase and K-feldspar coexist at the thermodynamic equilibrium (see Table 3EA). These feldspar-liquid pairs were used as test data for the plagioclase-liquid hygrometers of Putirka (2005, 2008) and Lange et al. (2009), as well as for the new K-feldspar–liquid hygrometer from this study. Note that we do not present results from the hygrometer of Putirka (2005) due the fact that the author found a systematic overestimate of ~1.3 wt.% H_2O compared with the more precise equation of Putirka (2008). The use of plagioclases from trachytic and phonolitic magmas as test data for the model of Lange et al. (2009) reveals some discrepancies between measured and calculated H_2O contents. Fig. 4a shows that the linear regression analysis yields lower correlation coefficient and higher uncertainty (R^2 = 0.72 and SEE = 1.15 wt.% H_2O) with respect to the good calibration statistics obtained by the authors (R^2 = 0.98 and SEE = 0.32 wt.% H_2O). Similar correlation coefficient and uncertainty (R^2 = 0.80 and SEE = 1.10 wt.% H_2O; Fig. 4a) are also recovered for the model of Putirka (2008) although its original calibration statistics (R^2 = 0.92 and SEE = 1.10 wt.% H_2O) are inferior to those of the hygrometer

of Lange et al. (2009). Therefore, the ability prediction of both plagioclase-liquid hygrometers is virtually identical for alkaline differentiated magmas, irrespective of the very different calibration strategy adopted by the authors to derive their models. Moreover, Fig. 4b shows that the statistics of predicted versus measured values of Eqn. (1) do not differ from those of previous hygrometers, showing only little improvements (R^2 = 0.82 and SEE = 0.94 wt.% H_2O). This means that the predictive power of the K-feldspar-liquid hygrometer is comparable to that of plagioclase-liquid models derived by Putirka (2008) and Lange et al. (2009) through the use of phase equilibrium experiments and standard-state thermodynamic data, respectively. Clearly, the advantage in using our model is due to the scarcity of plagioclase in alkaline differentiated products that makes very difficult to obtain a number of statistically significant H_2O estimates (Andujar et al., 2008, 2010; Andujar and Scaillet 2012). The formation of plagioclase is also frequently suppressed in phonolites that, in turn, contain abundant K-feldspar phenocrysts (e.g., Ablay et al., 1995; Fulignati et al., 2004).

3.3 K-feldspar–liquid equilibrium model

A crucial issue for mineral-liquid thermometers, barometers and hygrometers is undoubtedly the achievement of equilibrium between natural crystals and their host melts (Mollo et al., 2011a; Mollo and Masotta 2014). In the case of olivine and clinopyroxene, petrologists frequently test for equilibrium by means of the almost constant value of $^{xls\text{-}liq}Kd_{Fe\text{-}Mg}$ (Roeder and Emslie 1970; Putirka et al. 2003). More accurate equilibrium models were also derived for clinopyroxene through the difference between components predicted for clinopyroxene via regression analyses of equilibrium clinopyroxene-liquid pairs, with those measured in the analyzed natural crystals (Putirka 1999, 2008; Mollo et al. 2013). For plagioclase, Putirka (2008) pointed out that $^{plg\text{-}liq}Kd_{Or\text{-}Ab}$ is too dependent on the crystallization conditions of the system to be a useful test for equilibrium but he found good results for $^{plg\text{-}liq}Kd_{Ab\text{-}An}$. This model has been also successfully tested to predict equilibrium crystallization of plagioclase from alkaline and calc-alkaline magmas (Mollo et al.,

2011b, 2012; Lanzafame et al., 2013). According to the early finding of Putirka (2008), we have examined the behaviour of both Ab-An and Or-Ab exchange between K-feldspar and liquid. Contrary to what was observed for plagioclase, the relatively low amount of An in K-feldspar makes $^{kfs\text{-}liq}Kd_{Ab\text{-}An}$ unsuitable to test for equilibrium, whereas the abundance of Or and Ab components allows to successfully calibrate the following regression model:

$$^{kfs-liq}Kd_{Or-Ab} = a + d\left[\frac{Or^{liq}}{(Or^2)^{kfs}}\right] + e\ln\left[\frac{Or^2}{(Or+Ab)}\right]^{kfs}$$

(Eqn. 2)

Fig. 5a shows the good alignment between measured and predicted $^{kfs\text{-}liq}Kd_{Or\text{-}Ab}$ values, in agreement with the regression coefficients reported in Table 2. The effect of the independent variables on $Kd_{Or\text{-}Ab}$ is almost equivalent and close to ~50% for each single parameter. As for the case of hygrometer, we verified the accuracy of Eqn. (2) by means of compositions not included into the calibration dataset and coming from phase equilibrium experiments and MELTS simulations (Table 1EA). Most of the K-feldspar-liquid pairs obtained in laboratory are captured by Eqn. (2) suggesting near-equilibrium crystallization conditions for the experimental charges (Figs. 5b). Although $^{kfs\text{-}liq}Kd_{Or\text{-}Ab}$ from MELTS simulations are relatively low due to the fact that the algorithm does not account for the formation of anorthoclase, Eqn. (2) performs well with the thermodynamically-derived sanidine and liquid compositions (Fig. 5c). Given the convergence between our equilibrium model and MELTS data, the recalibrated Eqn. (2) shows regression-derived coefficients comparable to those of the original model (Fig. 5d and Table 2).

4. Application to the natural case study of Phlegrean Fields

The Phlegrean Fields (Italy) is one of the most dangerous volcanic complexes on Earth, owing to the intense urbanization within the caldera and its surroundings. The volcanic rocks

include compositions prevalently from shoshonite to peralkaline phonolite, with trachyte and alkali-trachyte as the most abundant (Pappalardo et al., 1999 and references therein). Different hypothesis have been proposed to explain the dynamics of the plumbing system, but the most recent suggest uprising of felsic liquids from a large, zoned magmatic reservoir (e.g., Pappalardo and Mastrolorenzo, 2012). Results from least-squared mass-balance calculations indicate that these evolved liquids formed through fractional crystallization from a more mafic parental magma, likely emplaced at 8 km depth (D'Antonio 2011). Seismic reflections corroborates the presence of a seismic discontinuity at 7.5 km in depth, whose seismic velocities are consistent with values expected for a magma body set in a densely fractured volume of rock (Zollo et al., 2008). Generally, melt inclusion data predict crystallization temperatures of magmas between 870 and 1080 °C (Fulignati et al., 2004; Marianelli et al., 2006). Thermometers specific to alkaline differentiated melts estimate crystallization temperatures for clinopyroxene in the range 884-983 °C (Masotta et al., 2013), whereas slightly lower temperatures of 840-960 °C are calculated by means of feldspar-liquid equilibria (Fedele et al., 2009).

To estimate the amount of H_2O dissolved in trachyte and phonolite magmas at the Phlegrean Fields, we have collected from literature a number of K-feldspar–liquid pairs representative of the caldera-forming eruptions of the Campanian Ignimbrite (CI) and Neapolitan Yellow Tuff (NYT), and some most recent eruptions (RE) occurred between 15 and 3.8 ka ago (Melluso et al., 1995; Orsi et al., 1995, Civetta et al., 1997; D'Oriano et al., 2005; Piochi et al., 2005, 2008; Fedele et al., 2008; Pappalardo et al., 2008; Fourmentraux et al., 2012). We have also integrated the dataset with additional analyses from this study (see Table 4EA for the whole dataset and the analytical conditions). Samples were grouped as pre-CI, CI, post-CI, NYT, and RE and were tested for equilibrium using Eqn. (2). Fig. 6a shows that the majority of compositions approach to the equilibrium one-to-one line, whereas a number of data from CI, NYT, and RE monotonically deviate from the equilibrium condition. The compositions plotting within 10 % of the one-to-one line yield fairly constant H_2O predictions that are assumed as reliable estimates (Fig. 6a). After the

screening of disequilibrium data, we have used Eqn. (1) to estimate the melt-H_2O content at 825 °C that is the optimum crystallization temperature of K-feldspar predicted by thermodynamic modelling (Fowler et al., 2007). Considering that the uncertainty of our new hygrometer is ~0.7 wt.% H_2O, all of the magmas at the Phlegrean Fields show comparable H_2O contents (Fig. 6b). However, we found ~4 wt.% range of H_2O contents in magma feeding pre-CI, CI, and post-CI eruptions, whereas the range lowers to ~2 wt.% H_2O for the NYT and RE products (Fig. 6b). These estimates agree with melt inclusion data suggesting H_2O concentrations between 3 and 6 wt.% for the original undegassed magma (Signorelli et al., 2001; Marianelli et al., 2006; Cannatelli et al., 2007; Mangiacapra et al., 2008; Esposito et al., 2011). Our predictions account also for the occurrence of multiple discrete populations of feldspar and glass in a single eruptive unit testifying to the heterogeneity of the magmatic system (cf. Mollo and Masotta 2014). Generally, magmas emplaced in the upper crust and feeding voluminous, explosive eruptions have a complex and protracted evolution (e.g., Bachmann and Bergantz, 2006). Under such circumstances, even fairly homogeneous eruptions may show ~2 wt.% range of H_2O caused by different processes, such as crystallization and depressurization at vapour-saturated conditions, closed system-degassing, and periodic gas fluxing from a subjacent more mafic reservoir (Bachmann et al., 2009). The higher melt-H_2O contents measured for magmas at Phlegrean Fields may reflect H_2O-saturated conditions prior to eruption. Thermo-dynamical models (Pappalardo et al., 2008) and experiments (Fabbrizio and Carroll, 2008) have demonstrated that H_2O-saturated magmas are capable of generating critical conditions of over-pressurisation in the chamber. Using the model of Papale et al. (2006), we have determined that the maximum H_2O solubility for the most evolved glass composition is 6.14 wt.%, in agreement with the highest H_2O content of 6.05 wt.% predicted by our hygrometer (Fig. 6b). Conversely, the relatively low concentration of H_2O measured in some melt inclusions and recovered by the new hygrometer may be the consequence of eruption-induced decompression events. As pressure is released during eruption, the volatile saturation level will drop deeper in the magmatic column, depleting magmas in volatiles (Bachmann et al., 2011 and references therein).

The amounts of dissolved H_2O in primitive CI melt inclusions (<3 wt.% H_2O) and matrix glasses (<1 wt.% H_2O) indicate strong H_2O degassing during ascent from the magma chamber toward the surface, with remarkable gas loss at shallow depths (1.1-1.6 km) and in the conduit (<0.8 km) (Pappalardo and Mastrolorenzo, 2012 and references therein). The empirical model of Papale et al. (2006) predicts that the solubility of H_2O in magma increases from 4.10 to 6.14 wt.% as the temperature decreases from 1150 to 850 °C at 0.15 GPa. MELTS runs performed by Fowler et al. (2007) at the same pressure corroborate these predictions, emphasizing that CI magma is H_2O-saturated at 1127 °C and 4.4 wt.% H_2O, and that the dissolved H_2O content continues to increase at the rate of 1 wt.% H_2O per 50 °C as heat is extracted and crystals precipitate. While H_2O-poor primitive melt inclusions are entrapped in olivine and clinopyroxene at relative high temperatures (1230 and 1160 °C, respectively), K-feldspar forms at the late stage of differentiation (<880 °C) under increasing H_2O concentration conditions (Fowler et al., 2007). In fact, the crystallization of K-feldspar coincides with a pseudo-invariant point where the fraction of melt remaining in the system significantly decreases from 0.5 to <0.1 leading to changes in the chemical composition (namely, dissolved H_2O content), and physical state (density, viscosity, volume fraction fluid) of the magma, possibly setting the stage for highly explosive eruptions (Fowler et al., 2007). This behaviour clearly remarks the importance of K-feldspar–liquid hygrometers for deciphering the evolution of H_2O in alkaline differentiated magmas prior to the onset of voluminous, caldera-forming eruptions.

Conclusions

We have calibrated and tested a new K-feldspar–liquid hygrometer through the regression analysis of a dataset that strictly reproduce the compositional variability of alkaline differentiated magmas in nature. The new test for equilibrium presented in this study is also able to filter existing experimental data in order to minimize the error of estimate. To validate our models with, we have

estimated H_2O dissolved in eruptive products at the Phlegrean Fields. Results are consistent with those obtained by means of melt inclusion analysis and H_2O solubility modelling.

Acknowledgments

A. Cavallo is acknowledged for assistance during electron microprobe analysis. S. Mollo was supported by ERC Starting grant 259256 GLASS project. The research activities of the HP-HT laboratory of the INGV were supported by the European Observing System Infrastructure Project (EPOS). Parts of this research were supported by Swiss NSF fund # 200021-146268

References

Ablay GJ, Ernst GGJ, Marti J, Sparks RSJ (1995) The ~ 2 ka subplinian eruption of Montaña Blanca, Tenerife. Journal of Volcanology and Geothermal Research 57:337-355

Andujar J, Costa F, Marti J (2010) Magma sotrage conditions of the last eruption of Teide volcano (Canary Island, Spain). Bulletin of Volcanology 72:381-395

Andujar J, Costa F, Marti J, Wolff JA, Carroll MR (2008) Experimental constraints on the pre-eruptive conditions of the phonolitic magma from the caldera-forming the Abrigo eruption, Tenerife (Canary Islands). Chem Geol 257(3-4):173-194

Andujar J, Scaillet B (2012) Relationships between pre-eruptive conditions and eruptive styles of phonolite-trachyte magmas. Lithos 152:122-131

Armienti P, Perinelli P, Putirka K (2013) A new model to estimate deep-level magma ascent rates, with applications to Mt. Etna (Sicily, Italy). Journal of Petrology 54:795-813

Bachmann O, Deering CD, Ruprecht JS, Huber C, Skopelitis A, Schnyder C (2011) Evolution of silicic magmas in the Kos-Nisyros volcanic center, Greece: a petrological cycle associated with caldera collapse. Contrib Mineral Petr 163(1):151-166

Bachmann O, Wallace P, Bourquin J (2009) The melt inclusion record from the rhyolitic Kos Plateau Tuff (Aegean Arc). Contributions to Mineralogy and Petrology 159(2):187-202

Bachmann O, Bergantz G W (2006) Gas percolation in upper-crustal silicic crystal mushes as a mechanism for upward heat advection and rejuvenation of near-solidus magma bodies. Journal of Volcanology and Geothermal Research 149:85– 102

Bowen N L (1937), Recent high-temperature research on silicates and its significance in igneous petrology. American Journal of Science, 33, 1-21.

Cannatelli C, Lima A, Bodnar RJ, De Vivo B, Webster JD, Fedele L (2007) Geochemistry of melt inclusions from the Fondo Riccio and Minopoli 1 eruptions at Campi Flegrei (Italy). Chem Geol 237(3-4):418-432

Civetta L, Orsi G, Pappalardo L, Fisher RV, Heiken G, Ort M (1997) Geochemical zoning, mingling, eruptive dynamics and depositional processes - The Campanian Ignimbrite, Campi Flegrei caldera, Italy. Journal of Volcanology and Geothermal Research 75(3-4):183-219

D'Antonio M (2011) Lithology of the basement underlying the Campi Flegrei caldera: Volcanological and petrological constraints. Journal of Volcanology and Geothermal Research 200(1-2):91-98

D'Oriano C, Poggianti E, Bertagnini A, Cioni R, Landi P, Polacci M, Rosi M (2005) Changes in eruptive style during the AD 1538 Monte Nuovo eruption (Phlegrean Fields, Italy): the role of syn-eruptive crystallization. Bulletin of Volcanology 67(7):601-621

Di Carlo I., Rotolo S.G., Scaillet B., Buccheri V. and Pichavant M. (2010) Phase equilibrium constraints on pre-eruptive conditions of recent felsic explosive volcanism at Pantelleria Island, Italy. Journal of Petrology, 51, 2245-2276.

Esposito R, Bodnar RJ, Danyushevsky LV, De Vivo B, Fedele L, Hunter J, Lima A, Shimizu N (2011) Volatile Evolution of Magma Associated with the Solchiaro Eruption in the Phlegrean Volcanic District (Italy). J Petrol 52(12):2431-2460

Fabbrizio A, Carroll MR (2008) Experimental constraints on the differentiation process and pre-emptive conditions in the magmatic system of Phlegraean Fields (Naples, Italy). Journal of Volcanology and Geothermal Research 171(1-2):88-102

Falloon T J, Green D H, O'Neill H St C, Hibberson W O (1997) Experimental tests of low degree peridotite partial melt compositions, implications for the nature of anhydrous near-solidus peridotite melts at 1GPa. Earth and Planetary Science Letters 152:149-162

Fedele L, Scarpati C, Lanphere M, Melluso L, Morra V, Perrotta A, Ricci G (2008) The Breccia Museo formation, Campi Flegrei, Southern Italy: Geochronology, chemostratigraphy and relationship with the Campanian Ignimbrite eruption. Bulletin of Volcanology 70(10):1189-1219

Fedele L, Zanetti A, Morra V, Lustrino M, Melluso L, Vannucci R (2009) Clinopyroxene/liquid trace element partitioning in natural trachyte-trachyphonolite systems: insights from Campi Flegrei (southern Italy). Contrib Mineral Petr 158(3):337-356

Forneris JF, Holloway JR (2003) Phase equilibria in subducting basaltic crust: implications for H(2)O release from the slab. Earth Planet Sc Lett 214(1-2):187-201

Fourmentraux C, Metrich N, Bertagnini A, Rosi M (2012) Crystal fractionation, magma step ascent, and syn-eruptive mingling: the Averno 2 eruption (Phlegraean Fields, Italy). Contrib Mineral Petr 163(6):1121-1137

Fowler SJ, Spera F, Bohrson W, Belkin HE, De Vivo B (2007) Phase equilibria constraints on the chemical and physical evolution of the campanian ignimbrite. J Petrol 48(3):459-493

Fulignati P, Marianelli P, Proto M, Sbrana A (2004) Evidences for disruption of a crystallizing front in a magma chamber during caldera collapse: an example from the Breccia Museo unit (Campanian Ignimbrite eruption, Italy). Journal of Volcanology and Geothermal Research 133:141-155

Ghiorso MS, Sack RO (1995) Chemical Mass-Transfer in Magmatic Processes .4. A Revised and Internally Consistent Thermodynamic Model for the Interpolation and Extrapolation of Liquid-Solid Equilibria in Magmatic Systems at Elevated-Temperatures and Pressures. Contrib Mineral Petr 119(2-3):197-212

Hamilton D L, MacKenzie W S (1965) Phase-equilibrium studies in the system $NaAlSiO_4$ (Nepheline)-$KAlSiO_4$ (Kalsilite)-SiO_2-H_2O. Mineralogical Magazine 34(268):214-231

Holtz F, Johannes W, Tamic N, Behrens H (2001) Maximum and minimum water contents of granitic melts generated in the crust: a reevaluation and implications. Lithos 56:1-14

Housh TB, Luhr JF (1991) Plagioclase-melt equilibria in hydrous systems. American Mineralogist 76:477-492

Jefferys WH, Berger JO (1992) Ockham Razor and Bayesian-Analysis. Am Sci 80(1):64-72

Lange RA, Frey HM, Jakob H (2009) A thermodynamic model for the plagioclase-liquid hygrometer/thermometer. American Mineralogist 94:494-506

Lanzafame G, Mollo S, Iezzi G, Ferlito C, Ventura G (2013) Unraveling the solidification path of a pahoehoe "cicirara" lava from Mount Etna volcano. Bulletin of Volcanology 75(4):703-719

Liu M, Yund R A (1992) NaSi–CaAl interdiffusion in plagioclase. American Mineralogist 77:275–283

Mangiacapra A, Moretti R, Rutherford M, Civetta L, Orsi G, Papale P (2008) The deep magmatic system of the Campi Flegrei caldera (Italy). Geophys Res Lett 35(21) doi:Artn L21304 Doi 10.1029/2008gl035550

Marianelli P, Sbrana A, Proto M (2006) Magma chamber of the Campi Flegrei supervolcano at the time of eruption of the Campanian Ignimbrite. Geology 34(11):937-940

Masotta M, Gaeta M, Gozzi F, Marra F, Palladino DM, Sottili G (2010) H2O- and temperature-zoning in magma chambers: The example of the Tufo Giallo della Via Tiberina eruptions (Sabatini Volcanic District, central Italy). Lithos 118(1-2):119-130

Masotta M, Mollo S, Freda C, Gaeta M, Moore G (2013) Clinopyroxene-liquid thermometers and barometers specific to alkaline differentiated magmas. Contrib Mineral Petr 166(6):1545-1561

Melluso L, Morra V, Perrotta A, Scarpati C, Adabbo M (1995) The Eruption of the Breccia Museo (Campi-Flegrei, Italy) - Fractional Crystallization Processes in a Shallow, Zoned Magma Chamber and Implications for the Eruptive Dynamics. Journal of Volcanology and Geothermal Research 68(4):325-339

Mollo S, Gaeta M, Freda C, Di Rocco T, Misiti V, Scarlato P (2010a) Carbonate assimilation in magmas: A reappraisal based on experimental petrology. Lithos 114:503-514

Mollo S, Del Gaudio P, Ventura G, Iezzi G, Scarlato P (2010b) Dependence of clinopyroxene composition on cooling rate in basaltic magmas: Implications for thermobarometry. Lithos 118:302-312

Mollo S, Putirka K, Iezzi G, Del Gaudio P, Scarlato P (2011a) Plagioclase–melt (dis)equilibrium due to cooling dynamics: implications for thermometry, barometry and hygrometry. Lithos 125:221–235

Mollo S, Lanzafame G, Masotta M, Iezzi G, Ferlito C, Scarlato P (2011b) Cooling history of a dike as revealed by mineral chemistry: A case study from Mt. Etna volcano. Chemical Geology 283:261–273.

Mollo S, Misiti V, Scarlato P, Soligo M (2012) The role of cooling rate in the origin of high temperature phases at the chilled margin of magmatic intrusions. Chemical Geology 322-323:28-46.

Mollo S, Putirka K, Misiti V, Soligo M, Scarlato P (2013) A new test for equilibrium based on clinopyroxene-melt pairs: Clues on the solidification temperatures of Etnean alkaline melts at post-eruptive conditions. Chemical Geology 352:92-100.

Mollo S, Masotta M (2014) Optimizing pre-eruptive temperature estimates in thermally and chemically zoned magma chambers. Chemical Geology 368:97-103.

Moore G, Carmichael ISE (1998) The hydrous phase equilibria (to 3 kbar) of an andesite and basaltic andesite from western Mexico: constraints on water content and conditions of phenocryst growth. Contrib Mineral Petr 130(3-4):304-319

Orsi G, Civetta L, Dantonio M, Digirolamo P, Piochi M (1995) Step-Filling and Development of a 3-Layer Magma Chamber - the Neapolitan-Yellow-Tuff Case-History. Journal of Volcanology and Geothermal Research 67(4):291-312

Pabst S, Worner G, Civetta L, Tesoro R (2008) Magma chamber evolution prior to the Campanian Ignimbrite and Neapolitan Yellow Tuff eruptions (Campi Flegrei, Italy). Bulletin of Volcanology 70(8):961-976

Palladino D, Gaeta M, Giaccio B, Sottili G (2014) On the anatomy of magma chamber and caldera collapse: The example of trachy-phonolitic explosive eruptions of the Roman Province (central Italy). Journal of Volcanology and Geothermal Research 281:12-26.

Papale P, Moretti R, Barbato D (2006) The compositional dependence of the saturation surface of $H_2O + CO_2$ fluids in silicate melts. Chemical Geology 229:78-95

Pappalardo L, Mastrolorenzo G (2012) Rapid differentiation in a sill-like magma reservoir: a case study from the campi flegrei caldera. Sci Rep-Uk 2 doi:Artn 712 Doi 10.1038/Srep00712

Pappalardo L, Ottolini L, Mastrolorenzo G (2008) The Campanian Ignimbrite (southern Italy) geochemical zoning: insight on the generation of a super-eruption from catastrophic differentiation and fast withdrawal. Contrib Mineral Petr 156(1):1-26

Pappalardo L, Piochi M, D'Antonio M, Civetta L, Petrini R (2002) Evidence for multi-stage magmatic evolution during the past 60 kyr at Campi Flegrei (Italy) deduced from Sr, Nd and Pb isotope data. J Petrol 43(8):1415-1434

Pappalardo L, Civetta L, D'Antonio M, Deino A, Di Vito M, Orsi G, Carandente A, de Vita S, Isaia R, Piochi M (1999) Chemical and Sr-isotopical evolution of the Phlegraean magmatic system before the Campanian Ignimbrite and the Neapolitan Yellow Tuff eruptions. Journal of Volcanology and Geothermal Research 91(2-4):141-166)

Piochi M, Mastrolorenzo G, Pappalardo L (2005) Magma ascent and eruptive processes from textural and compositional features of Monte Nuovo pyroclastic products, Campi Flegrei, Italy. Bulletin of Volcanology 67(7):663-678

Piochi M, Polacci M, De Astis G, Zanetti A, Mangiacapra A, Vannucci R, Giordano D (2008) Texture and composition of pumices and scoriae from the Campi Flegrei caldera (Italy):

Implications on the dynamics of explosive eruptions. Geochem Geophy Geosy 9 doi:Artn Q03013 Doi 10.1029/2007gc001746

Putirka K (1999) Clinopyroxene plus liquid equilibria to 100 kbar and 2450 K. Contrib Mineral Petr 135(2-3):151-163

Putirka K (2005) Igneous thermometers and barometers based on plagioclase+liquid equilibria: test of some existing models and new calibrations. American Mineralogist 90:336-346

Putirka K (2008) Thermometers and barometers for volcanic systems. Reviews in Mineralogy & Geochemistry 69:61-120

Putirka KD, Mikaelian H, Ryerson F, Shaw H (2003) New clinopyroxene-liquid thermobarometers for maric, evolved, and volatile-bearing lava compositions, with applications to lavas from Tibet and the Snake River Plain, Idaho. American Mineralogist 88(10):1542-1554

Ratkowsky DA (1990) Handbook of non-linear regression models. Marcel Decker Inc., New York

Roeder PL, Emslie RF (1970) Olivine-Liquid Equilibrium. Contrib Mineral Petr 29(4):275-289

Scaillet B, Macdonald R (2003) Experimental constraints on the relationships between peralkaline rhyolites of the Kenya rift valley. J Petrol 44(10):1867-1894

Signorelli S, Vaggelli G, Romano C, Carroll MR (2001) Volatile element zonation in Campanian Ignimbrite magmas (Phlegrean Fields, Italy): evidence from the study of glass inclusions and matrix glasses. Contrib Mineral Petr 140(5):543-553

Zollo A, Maercklin N, Vassallo M, Dello Iacono D, Virieux J, Gasparini P (2008) Seismic reflections reveal a massive melt layer feeding Campi Flegrei caldera. Geophys Res Lett 35(12) doi:Artn L12306 Doi 10.1029/2008gl034242

Figure captions

Fig. 1. Total alkali versus silica diagram (a) and ternary phase diagram for the system Or-Ab-An (b) showing liquids and K-feldspars from the alkaline dataset, respectively.

Fig. 2. Eqn. (1) was calibrated through the regression analysis of experimental data (a) and then was tested by using experimental compositions external to the calibration dataset (b) as well as thermodynamic compositions from MELTS runs (c). The ability prediction of Eqn. (1) recalibrated by using both experimental and MELTS data does not differ from that of the original model (d).

Fig. 3. The error of water estimate (EWE) due to the use of Eqn. (1) increases with increasing $[Si/(Na+K)]^{liq}$. While K-feldspar–liquid pairs from trachytes and phonolites show relatively low EWE, this does not apply to rhyolites characterized by the occurrence of compositionally different K-feldspar–liquid pairs that are external to the calibration dataset.

Fig. 4. We used as test data for previous plagioclase-liquid hygrometers of Putirka (2005, 2008) and Lange et al. (2009) (a) and for the new K-feldspar–liquid hygrometer (b), MELTS runs in which both plagioclase and K-feldspar coprecipitated from the same alkaline liquid under identical P-T-X-H_2O conditions. Results demonstrate that our model offers the same accurate predictions measured for other hygrometers with the advantage that K-feldspar is the most abundant and H_2O-sensitive phase in trachyte and phonolite products.

Fig. 5. $^{kfs\text{-}liq}Kd_{Or\text{-}Ab}$ is a new test for equilibrium, i.e., Eqn. (2), based on Or-Ab exchange between K-feldspar and liquid (a). The accuracy of Eqn. (2) has been tested by using as input data some experimental compositions external to the calibration dataset (b) and thermodynamic compositions from MELTS runs (c). The ability prediction of Eqn. (2) recalibrated by using both experimental and MELTS data does not differ from that of the original model (d).

Fig. 6. K-feldspar–liquid pairs from products of the Phlegrean Fields were used as input data for our new models. First, we have tested for equilibrium through Eqn. (2), assuming as reliable the

compositions plotting within 10 % of the one-to-one line and yielding almost constant H_2O predictions (a). Second, after the screening of disequilibrium data, we have used Eqn. (1) to estimate the melt-H_2O content (b). Our estimates are consistent with results from H_2O solubility modelling and a number of previous melt inclusion data measuring comparable H_2O concentrations for both primitive and more evolved magmas. Pre-CI: pre-Campanian Ignimbrite eruptions. CI: Campanian Ignimbrite eruption. Post-CI: post-Campanian Ignimbrite eruptions. NYT: Neapolitan Yellow Tuff eruption. RE: recent eruptions.

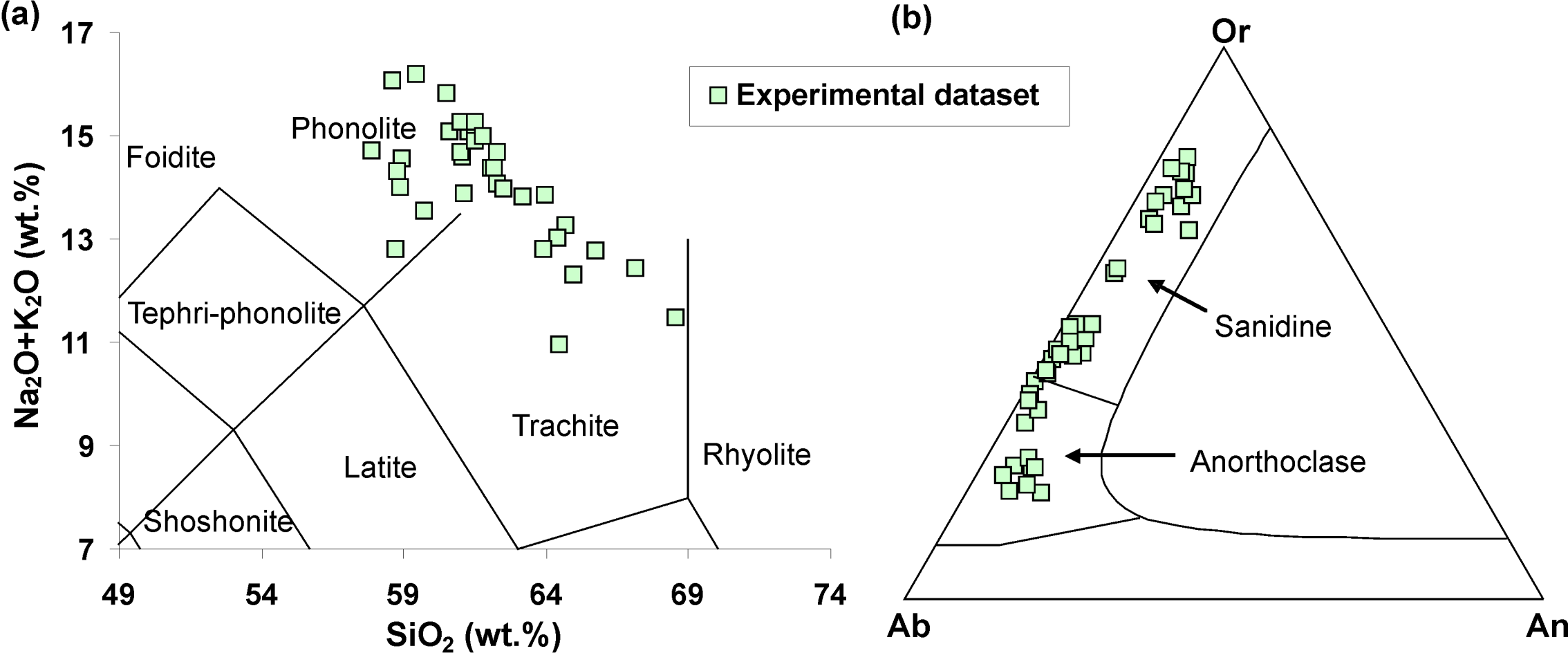
(a)
17
15
13
11
9
7
Na2O+K2O (wt.%)
49
54
59
64
69
74
SiO2 (wt.%)
Foidite
Phonolite
Tephri-phonolite
Trachite
Rhyolite
Latite
Shoshonite
Experimental dataset
(b)
Or
Ab
An
Sanidine
Anorthoclase

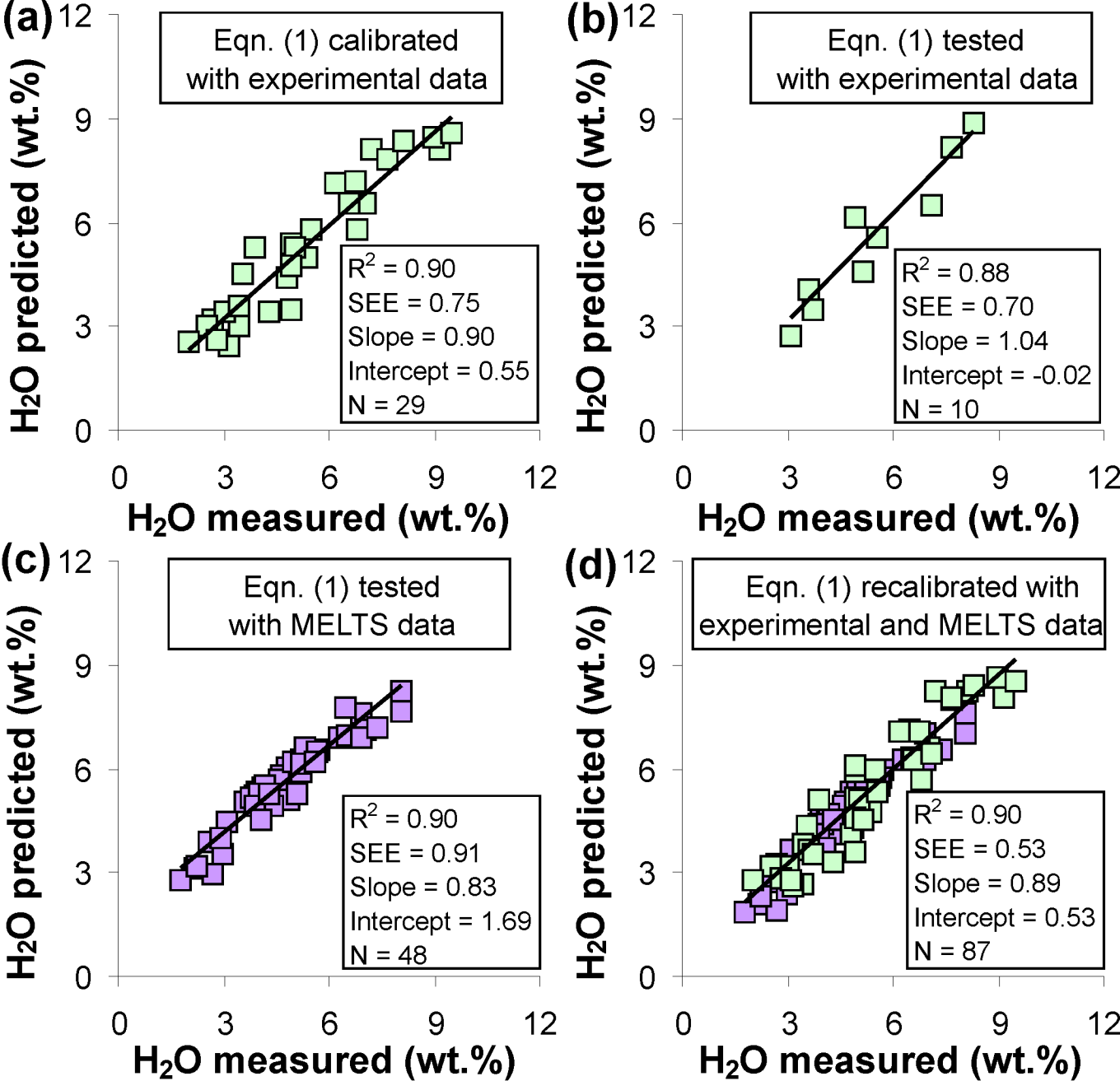
(a)
Eqn. (1) calibrated with experimental data
R2 = 0.90
SEE = 0.75
Slope = 0.90
Intercept = 0.55
N = 29
H2O predicted (wt.%)
H2O measured (wt.%)
(b)
Eqn. (1) tested with experimental data
R2 = 0.88
SEE = 0.70
Slope = 1.04
Intercept = -0.02
N = 10
H2O predicted (wt.%)
H2O measured (wt.%)
(c)
Eqn. (1) tested with MELTS data
R2 = 0.90
SEE = 0.91
Slope = 0.83
Intercept = 1.69
N = 48
H2O predicted (wt.%)
H2O measured (wt.%)
(d)
Eqn. (1) recalibrated with experimental and MELTS data
R2 = 0.90
SEE = 0.53
Slope = 0.89
Intercept = 0.53
N = 87
H2O predicted (wt.%)
H2O measured (wt.%)
0
3
6
9
12

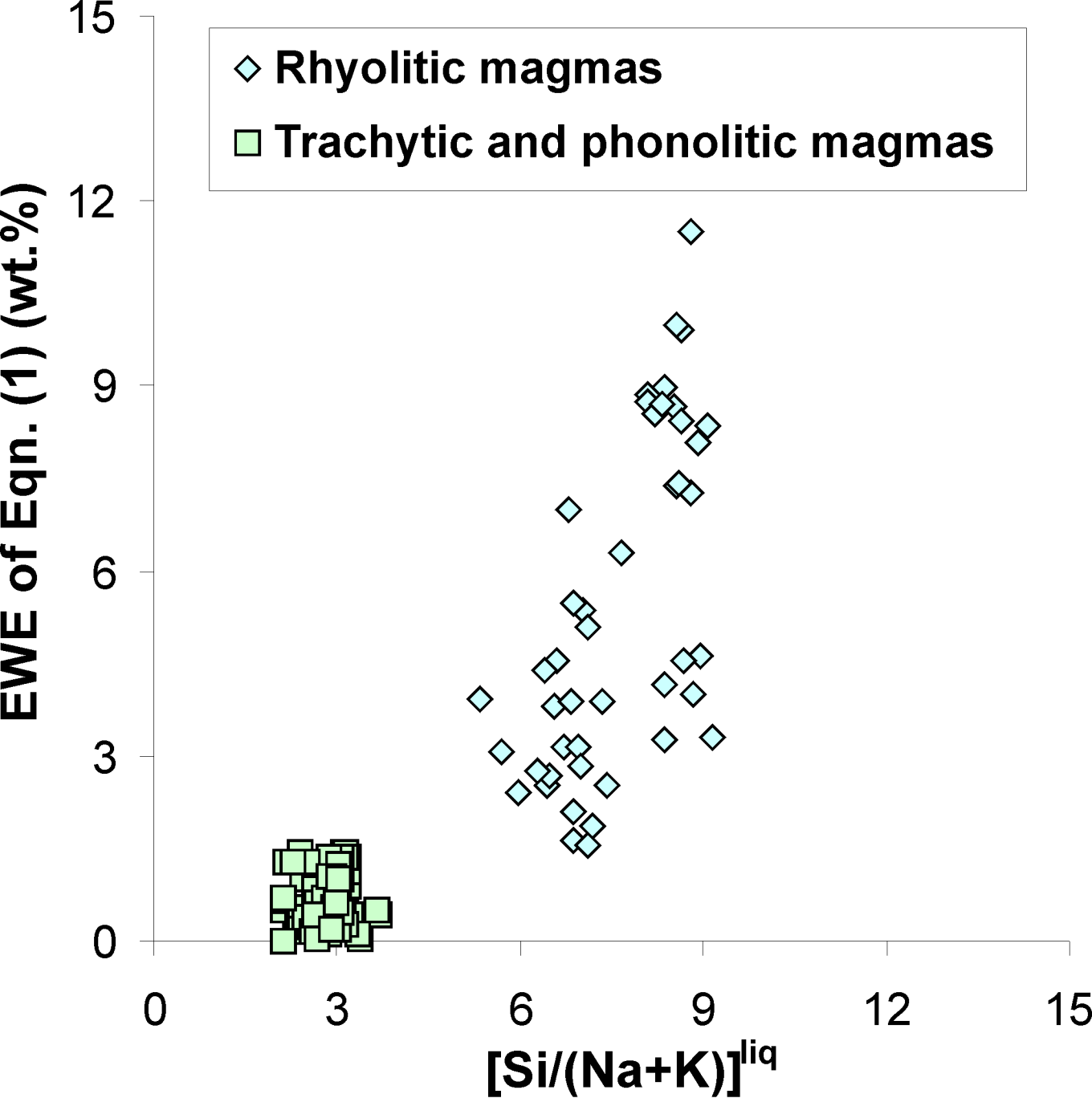
Rhyolitic magmas
Trachytic and phonolitic magmas
EWE of Eqn. (1) (wt.%)
[Si/(Na+K)]liq
0
3
6
9
12
15

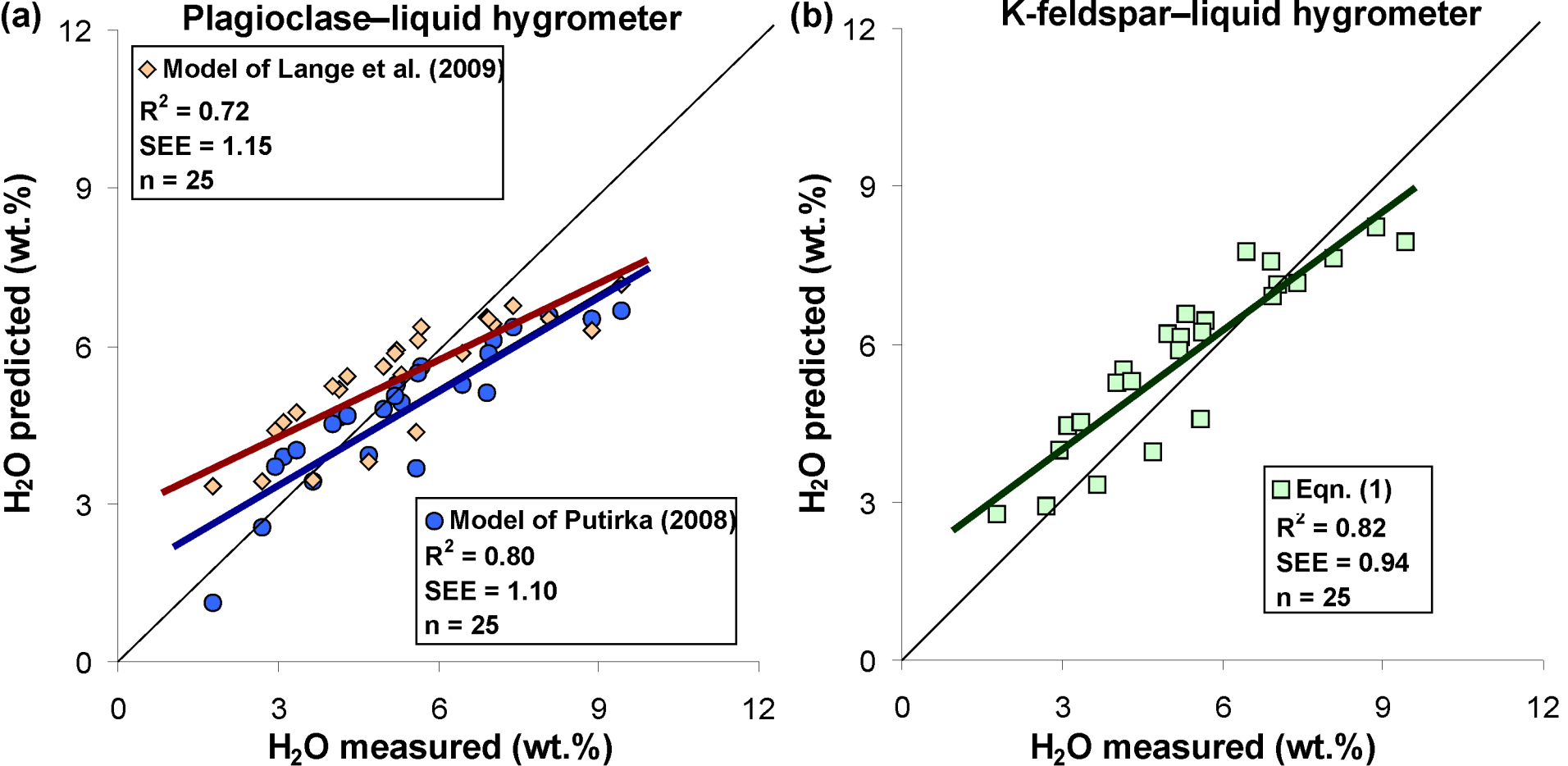
(a)
Plagioclase–liquid hygrometer
Model of Lange et al. (2009)
R2 = 0.72
SEE = 1.15
n = 25
Model of Putirka (2008)
R2 = 0.80
SEE = 1.10
n = 25
H2O predicted (wt.%)
H2O measured (wt.%)
0
3
6
9
12
(b)
K-feldspar–liquid hygrometer
Eqn. (1)
R2 = 0.82
SEE = 0.94
n = 25
H2O predicted (wt.%)
H2O measured (wt.%)

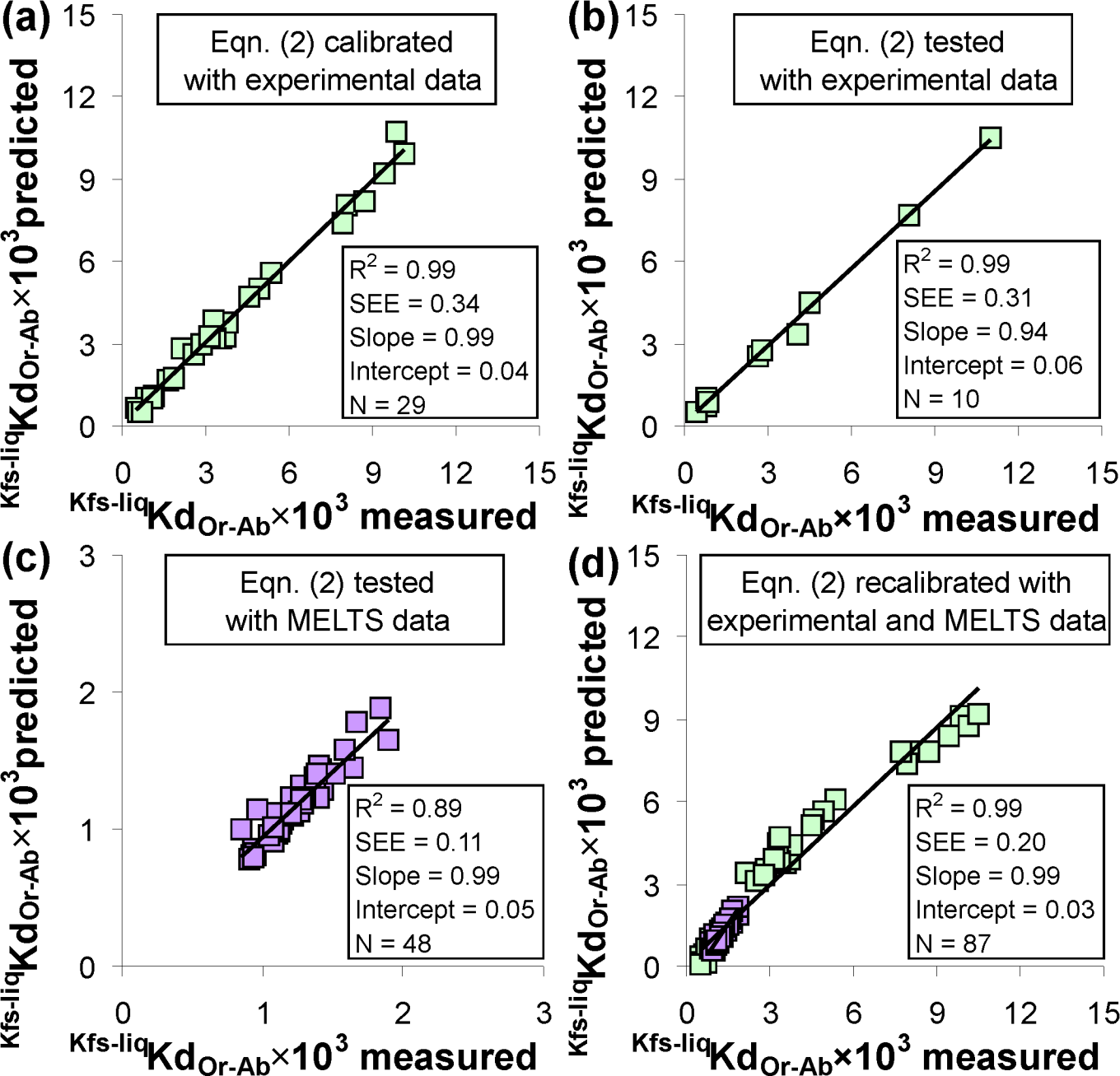
(a)
Eqn. (2) calibrated with experimental data
R^2 = 0.99
SEE = 0.34
Slope = 0.99
Intercept = 0.04
N = 29
$^{Kfs-liq}Kd_{Or-Ab}\times10^3$ predicted
$^{Kfs-liq}Kd_{Or-Ab}\times10^3$ measured
(b)
Eqn. (2) tested with experimental data
R^2 = 0.99
SEE = 0.31
Slope = 0.94
Intercept = 0.06
N = 10
$^{Kfs-liq}Kd_{Or-Ab}\times10^3$ predicted
$^{Kfs-liq}Kd_{Or-Ab}\times10^3$ measured
(c)
Eqn. (2) tested with MELTS data
R^2 = 0.89
SEE = 0.11
Slope = 0.99
Intercept = 0.05
N = 48
$^{Kfs-liq}Kd_{Or-Ab}\times10^3$ predicted
$^{Kfs-liq}Kd_{Or-Ab}\times10^3$ measured
(d)
Eqn. (2) recalibrated with experimental and MELTS data
R^2 = 0.99
SEE = 0.20
Slope = 0.99
Intercept = 0.03
N = 87
$^{Kfs-liq}Kd_{Or-Ab}\times10^3$ predicted
$^{Kfs-liq}Kd_{Or-Ab}\times10^3$ measured

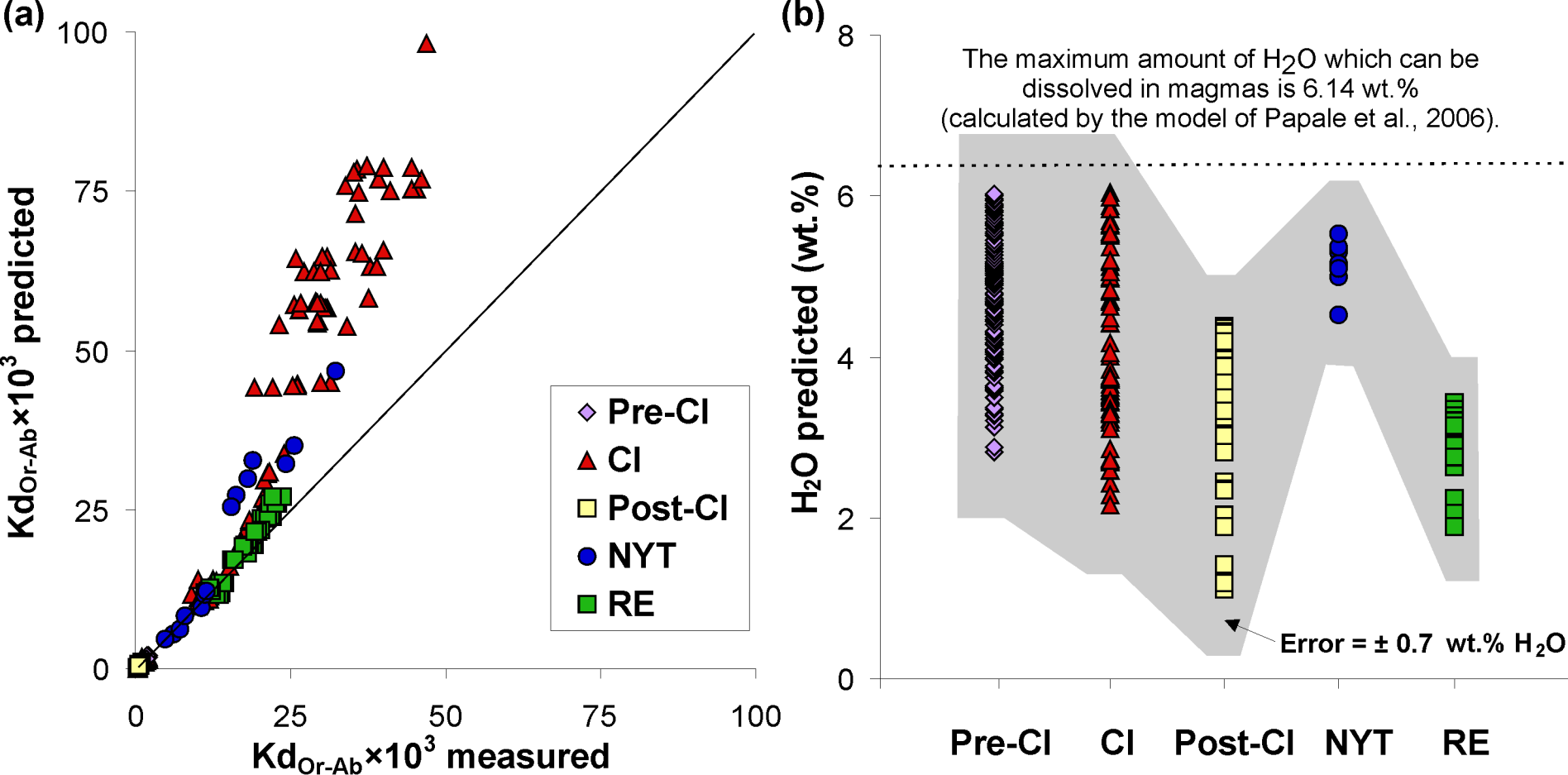
(a)
100
75
50
25
0
0
25
50
75
100
$Kd_{Or-Ab}\times10^3$ predicted
$Kd_{Or-Ab}\times10^3$ measured
Pre-CI
CI
Post-CI
NYT
RE
(b)
8
6
4
2
0
H_2O predicted (wt.%)
The maximum amount of H_2O which can be dissolved in magmas is 6.14 wt.% (calculated by the model of Papale et al., 2006).
Error = ± 0.7 wt.% H_2O
Pre-CI
CI
Post-CI
NYT
RE

Table 1. In order to find regression parameters with high correlation coefficients (R) and low standard errors of estimate (SEE), the concentration of H_2O dissolved in the melt is compared with the cation fractions of both liquid and feldspar components. The same strategy is used for the Or-Ab exchange between K-feldspar and liquid, i.e., $^{kfs\text{-}liq}Kd_{Or\text{-}Ab}$. The value of ±1σ refers to the uncertainty of the intercept and slop calculated for the regression equation, whereas sd refers to the standard deviation of both dependent and independent variables. Liq = liquid. Kfs = K-feldspar.

Dependent variable	Independent variable	Parameter	R^2	SEE	Intercept	±1σ	Slope	±1σ	Sd
H_2O (sd = 2.14)	P	P	0.01	2.05	4.88	0.84	2.52	4.38	0.08
	T	$10^4/T$	0.51	1.44	-12.81	2.91	1.48	0.24	0.99
	Liq	-ln(Si)	0.27	1.76	18.52	3.60	-21.86	5.95	0.05
		-ln(Ti)	0.53	1.41	-10.64	2.48	2.60	0.40	0.57
		-ln(Al)	0.00	2.06	3.86	10.94	0.94	6.99	0.05
		-ln(Fe)	0.00	2.06	5.02	1.48	0.06	0.30	1.12
		-ln(Mg)	0.58	1.34	-12.23	2.47	2.91	0.41	0.50
		-ln(Ca)	0.07	1.99	2.20	1.97	0.73	0.46	0.70
		-ln(Na)	0.00	2.06	5.14	2.43	0.10	1.19	0.28
		-ln(K)	0.07	1.99	-0.97	3.79	2.34	1.41	0.24
		-ln(SiMg)	0.63	1.26	-11.13	2.10	3.04	0.39	0.53
		-ln[Si(Ti+Mg)]	0.66	1.21	-16.59	2.61	3.67	0.44	0.45
		An	0.07	1.98	6.31	0.65	-12.82	7.45	0.04
		Ab	0.03	2.03	3.56	1.73	2.92	2.80	0.12
		Or	0.03	2.03	16.88	11.26	-10.00	9.74	0.03
	Kfs	-ln(Si)	0.24	1.80	44.60	11.59	-73.44	21.66	0.01
		-ln(Al)	0.01	2.05	-2.91	15.19	5.27	9.71	0.04
		-ln(Fe)	0.46	1.51	-8.05	2.38	2.45	0.43	0.56
		-ln(Ca)	0.18	1.86	-1.05	2.23	1.29	0.45	0.68
		-ln(Na)	0.01	2.05	4.20	1.63	0.45	0.64	0.52
		-ln(K)	0.17	1.88	9.94	1.73	-1.90	0.70	0.43
		$\ln(Si/Fe^2)$	0.47	1.50	-7.38	2.24	1.22	0.21	1.14
		$\ln[(SiCa)/(Fe+Ca)^2]$	0.59	1.32	-5.53	1.51	3.26	0.45	0.48
		An	0.27	1.76	7.06	0.54	-38.49	10.32	0.03
		Ab	0.06	2.00	6.47	0.84	-2.46	1.67	0.19
		Or	0.10	1.96	3.75	0.86	3.23	1.63	0.19
	Kfs-liq	$\ln[(Or^2)^{Kfs}/K^{liq})]$	0.40	1.60	1.66	0.79	3.96	0.80	0.32
		$\ln[(Or^2)^{Kfs}/(CaK)^{liq}]$	0.63	1.25	-5.95	1.43	2.11	0.26	0.77
		$\ln(An^{Kfs}/An^{liq})$	0.02	2.04	5.18	0.37	0.28	0.31	1.07
		$\ln(Ab^{Kfs}/Ab^{liq})$	0.11	1.95	4.62	0.46	2.03	0.96	0.33
		$\ln(Or^{Kfs}/Or^{liq})$	0.16	1.89	7.01	0.70	-1.77	0.67	0.46
$^{kfs\text{-}liq}Kd_{Or\text{-}Ab}$ (sd = 3.06)	Kfs-liq	$Or^{liq}/(Or^{kfs})^2$	0.95	0.74	0.61	0.15	0.36	0.01	0.87
	Kfs	$-\ln[Or^2/(Or+Ab)]$	0.95	0.69	-1.66	0.23	3.44	0.13	8.43

Table 2. We report results from multiple linear regression analyses conducted on experimental data to calibrate a new K-feldspar-liquid hygrometer, i.e., Eqn. (1), and a new equilibrium model for $^{kfs\text{-}liq}Kd_{Or\text{-}Ab}$, i.e., Eqn. (2). As a term of comparison, we also report the regression parameters derived for Eqns. (1) and (2) recalibrated through the regression analysis of experimental and MELTS data that were used to test the models and were not included into the original calibration dataset. The correlation coefficient (R) and standard error of estimate (SEE) do not show substantial variations for both the original and recalibrated models.

Eqn.	Dependent variable	Intercept		Independent variable								R^2	SEE
				Temperature		Liquid		K-feldspar-liquid		K-feldspar			
		a	±1σ	b	±1σ	c	±1σ	d	±1σ	e	±1σ		
(1)	H_2O	-18.49	1.25	0.86	0.21	0.74	0.57	1.02	0.36	1.03	0.45	0.90	0.75
Recal (1)		-19.52	0.88	0.84	0.10	1.23	0.21	0.98	0.16	0.59	0.09	0.90	0.53
(2)	$^{kfs\text{-}liq}Kd_{Or\text{-}Ab}$	-0.67	0.18	-	-	1.73	0.20	-	-	0.20	0.02	0.99	0.34
Recal (2)		-0.55	0.06	-	-	1.65	0.09	-	-	0.20	0.01	0.99	0.20